Glowing gold nanoparticle coating:

Restoring the lost property from bulk gold

Yukari Kawabe[a], Takashi Ito[b], Hiroaki Yoshida[c], Hiroshi Moriwaki*[a,b]

[a] Department of Applied Biology, Faculty of Textile Science and Technology, Shinshu University, 3-15-1 Tokida, Ueda 386-8567, Japan, e-mail: moriwaki@shinshu-u.ac.jp

[b] Research Center for Supports to Advanced Science, Division of Instrumental Analysis (Ueda branch), Shinshu University, 3-15-1 Tokida, Ueda 386-8567, Japan

[c] Department of Chemistry and Materials, Faculty of Textile Science and Technology, Shinshu University, 3-15-1 Tokida, Ueda 386-8567, Japan

ABSTRACT

The unique electronic, optical, and catalytic properties of AuNPs caused by localized surface plasmon resonance (LSPR) have attracted many scientists, but the LSPR diminishes the captivating luster of bulk gold. An exciting challenge is fabrication of golden-colored AuNPs, but a decisive factor for controlling the absorption/reflection of AuNPs remains elusive. We now propose a simple and versatile method for the fabrication of glowing AuNPs to restore the “lost golden color” of AuNPs by combination with the deposition of AuNPs on a cellulose filter or a PET/cotton fabric by the successive ionic layer adsorption and reaction (SILAR) method and simple pencil drawing. The obtained materials exhibited the glowing golden-color on the pencil-drawn surface and common red and blue colors on the other part. Surprisingly, the golden AuNPs still maintain a catalytic activity different from that of bulk gold and could be used as a catalyst for the reduction of *p*-nitrophenol, pendimethalin or 2,4-dinitrophenol in the presence of $NaBH_4$. We believe that re-endowment of such a property characteristic of bulk gold into gold nanomaterials would lead to further advancement in the arts and culture as well as electronics, optics, and catalysis.

Keywords: glowing gold nanoparticle, SILAR method, pencil graphite, catalytic activity, cellulose filter

Introduction

Over the past few decades, the rapid advancements in nanoscience and nanotechnology have produced many innovative materials and techniques.[1] A very important research area is the downsizing of bulk metals into nanometer-sized materials, such as nanoparticles and nanosheets, motivated by the appearance of electronic, electric, optical, thermal, and catalytic properties[2-6] due to the quantum size effect,[7] surface plasmon resonance (SPR),[8] and significantly increased surface area of the metal nanomaterials. Among them, gold nanoparticles (AuNPs) are an extensively-studied subject and show characteristic electronic and optical properties because of the localized SPR (LSPR) phenomenon, different from bulk gold.[9] Many nanosized gold constructs have been fabricated and received much attention in many fields, such as the environmental sciences,[10] analytical chemistry,[11] and medical sciences.[12] Although there are very promising and possible applications of gold nanomaterials, we have long overlooked the most-captivating, but lost property of gold nanomaterials from bulk gold, that is, “the glowing, golden color”. We believe that re-endowment of such a property characteristic of bulk gold into gold nanomaterials would lead to further advancement in the arts and culture as well as electronics, optics, and catalysis.

The unique “golden” color of bulk gold is recognized as a symbolic color which represents a kind of invariance, luxury, and nobleness, and appears as the result of the absorption of visible light with 2.4 eV corresponding to the electronic transition from the 5d to the 6s level.[13] In addition to this,

53 the good ductility and malleability of bulk gold have been responsible for the fabrication of historic
54 treasures and ornaments.[14] On the other hand, AuNPs usually show a red or blue color depending on
55 their particle sizes because of the LSPR effect, i.e., the oscillation of free electrons on the surface.[15]
56 The historic emergence of AuNPs dates back to the 4th-century Lycurgus Cup, and even at present,
57 the gold ruby glass stained with AuNPs and the ceramics painted with an AuNPs solution have been
58 fascinating.[16] There are also many publications on the coating of AuNPs onto various substrates, and
59 most of the obtained materials showed only red or blue.[17] To the best of our knowledge, very few
60 studies have ever tried to prepare glowing AuNPs. Ung et al. reported that the homogeneous films of
61 Au@SiO_2 particles deposited on glass using a layer-by-layer (LbL) self-assembly displayed a
62 metallic reflection close to bulk gold metal films.[18] Torrell et al. stated that AuNPs dispersed in an
63 amorphous TiO_2 dielectric matrix after annealing at 300 ºC exhibited a reflection similar to bulk gold
64 with a golden yellow color.[19,20] Amendola et al. reported that graphite-coated AuNPs significantly
65 suppresses the LSPR by laser ablation in toluene according to the Mie model.[21] However, those
66 materials and methods are not easy and the decisive factor for controlling the absorption and
67 reflection of AuNPs remains elusive, therefore, a facile and versatile approach should be proposed
68 for the realization of golden AuNP coatings for further applications.
69 In order to accomplish such a novel AuNP coating, two fundamental issues should be solved.
70 One is to use a suitable coating technique which allows the preparation of AuNPs on/in various

71 substrates at appropriate densities because the aggregation of AuNPs leads to a red-shift in the
72 absorption wavelength.[13] One of the satisfying approaches is the successive ionic layer adsorption
73 and reaction (SILAR) method.[22,23] This method is regarded as a technique related to the LbL
74 approaches[24] or alternate immersions[25] and offers the deposition of metal nanoparticles on/in a
75 variety of substrates by alternate immersion of a substrate into a metal ion solution and a reducing
76 agent solution.[26] In this study, we selected two general materials, cellulose filter papers (CF) and
77 PET/cotton fabrics, as the coating substrates of the AuNPs to demonstrate that our technique is
78 simple and versatile and can be used for various shaped substrates with different dimensions. The
79 other is how to suppress the LSPR of the coated AuNPs to get a metallic reflection on the material
80 surface. As shown above, the shielding or embedding of AuNPs in SiO_2, TiO_2, or graphite seems to
81 cause electronic interactions with the AuNPs, but such procedures are complicated.[19-21] Thus as a
82 simpler approach, we focused on pencil graphite (PG),[27] which can be decorated on the surface of
83 the materials simply by drawing or painting, and then the obtained composite of the AuNPs and
84 graphite was evaluated. Combination of the synthesis of AuNPs by the SILAR method and the
85 addition of PG interlayers would be a simple, but powerful approach to provide an AuNP-coated
86 surface with the glowing golden color (**Fig. 1**).
87

88 ## Experimental section

89 **Materials**

90 Sodium tetrachloroaurate ($NaAuCl_4$) dihydrate, ascorbic acid sodium salt, graphene nanoplatelets
91 aggregates, nitric acid, hydrochloric acid, methanol, and *p*-nitrophenol were obtained from
92 FUJIFILM Wako Pure Chemical Corporation (Osaka, Japan). Pendimethalin was purchased from
93 Tokyo Chemical Industry Co., Ltd. (Tokyo, Japan). 2,4-Dinitrophenol was from KANTO
94 CHEMICAL CO., INC. (Tokyo, Japan). Cellulose filter (CF: 5A, ϕ 55 mm) was from ADVANTEC
95 (Tokyo, Japan). The fabric (polyester 65%, cotton 35%) was obtained by cutting a laboratory coat.
96 The HB pencil from Chienotomo Pencil (Tokyo, Japan) and 6B pencil from Mitsubishi Pencil were
97 used for painting or drawing on the substrates.

98

99 **Deposition of AuNPs on/in CF by Combining SILAR Method with Pencil Drawing**

100 Both sides of CF were overall painted with a pencil by the cross-hatching method to prepare pencil
101 graphite (PG)-painted CF (PG/CF). The PG/CF was decorated with AuNPs by the SILAR method
102 which comprises of 4 steps. [1] Rinse the PG/CF with distilled water for 10 sec. [2] Immerse it in
103 $NaAuCl_4$ aq. (5.0 mM, 10 mL) for 10 sec. [3] Rinse it with distilled water. [4] Immerse in ascorbic
104 acid aq. (50 mM, 10 mL) for 10 sec (**Fig. 1**). The cycle from step 1 to step 4 was repeated 10 times.
105 Finally, the filter was freeze-dried overnight to get AuNPs on/in PG-painted CF (Au/PG/CF). The
106 sample prepared without pencil drawing was abbreviated as Au/CF.

Plasma-treated PG/CF was prepared by using a plasma generator (PIB-10, Vacuum Device, Ibaraki, Japan). The PG/CF was exposed by plasma in the presence of oxygen for 5 min at discharge current 8-16 mA.

Preparation of Gold Colloidal Aqueous Solution

$NaAuCl_4$ aq. (0.125 mM, 40 mL) was mixed with an ascorbic acid aq. (1.6 mM, 10 mL) to get colloidal suspension. The obtained mixture was dialyzed using a dialysis tube (MWCO: 14000, FUJIFILM Wako Pure Chemical Corporation, Osaka, Japan) for 12 hours to remove impurities. The obtained red solution was used as the gold colloidal solution.

Characterization of AuNPs

The sample filters were analyzed by an X-ray diffractometer (Mini Flex 300, Rigaku, Tokyo, Japan) for confirming the formation of the AuNPs and determining the crystalline forms. The sample (Au/PG/CF, Au/CF, PG/CF, or the untreated CF) was attached to the reflection-free stage and measured from 5^o to 80^o.

The gold quantities of the samples were determined by inductivity coupled plasma atomic emission spectrometry (ICP/AES, SPS3100, SII Nanotechnology, Tokyo, Japan). The gold was extracted by immersing the sample (1 cm × 1 cm) in royal water (HNO_3: HCl = 1:3) for 3 hours.

125 The surface of the samples was observed by a stereo microscope equipped with a CCD camera
126 (SZX7, Olympus, Tokyo, Japan). The AuNPs deposited on the surface of the CFs were investigated
127 by a FE-SEM (S-5000, Hitachi, Tokyo, Japan) after sputtered with platinum and palladium using an
128 E-1030 instrument (Hitachi, Tokyo, Japan). The AuNPs were also visualized using a TEM
129 (JEM-2100, Tokyo, Japan) at the operating voltage of 200 kV. The sample was scuffed by tweezers,
130 and the obtained cellulose fibers were placed on a Cu 200 mesh grid (JEOL, Tokyo, Japan) and used
131 for TEM observation. The distribution of the particle sizes of AuNPs was determined from the
132 obtained TEM images (n=100). The resistivity was measured by a low-resistivity meter (Loresta-GP
133 MCP-T6, DINS, Kanagawa, Japan) or a high-resistivity meter (Hiresta-UP, DINS, Kanagawa, Japan).
134 XPS measurements were performed by an AXIS-ULTRA^{DLD} spectrophotometer (Kratos Analytical
135 Ltd., UK), with Mg-Kα radiation.
136
137 **Catalytic Activities of CF or PG/CF with and without AuNPs**
138 The catalytic reaction from *p*-nitrophenol (*p*-NP) to *p*-aminophenol (*p*-AP) using the cellulose filters
139 (Au/PG/CF, Au/CF, PG/CF, and the untreated CF) as a catalyst with sodium borohydride ($NaBH_4$) as
140 a reducing agent was studied. The *p*-NP aq. (10 mL, 10 mg L^{-1}) was mixed with the $NaBH_4$ aq. (2.5
141 mL, 10 g L^{-1}) in the presence of the CF (1 cm x 1 cm). The mixture was stored for 1-28 h, and the
142 absorbance at 400 nm of the solution was measured. The absorbance was obtained by an absorption

143 spectrometer (V-630DS, JEOL, Tokyo, Japan).

144

145 **Catalytic reaction of herbicides using the Au/PG/CF**

146 The methanol solution of pendimethalin (10 mL, 100 mg L^{-1}) was mixed with the $NaBH_4$ aq. (2.5

147 mL, 10 g L^{-1}) in the presence of the Au/PG/CF (1 cm x 1 cm). In the case of 2,4-dinitrophenol, the

148 aqueous solution of 2,4-dinitrophenol (10 mL, 36.8 mg L^{-1}) was mixed with the $NaBH_4$ aq. (2.5 mL,

149 10 g L^{-1}) in the presence of the Au/PG/CF (1 cm x 1 cm). The mixture was stored for 5 h, and the

150 absorption spectrum (300-500 nm) of the solution was measured. The filtrate of the reaction mixture

151 was analyzed by electrospray ionization / mass spectrometry in positive ion mode using a LC/MS

152 2010A (Shimadzu, Kyoto, Japan) with a scan range of *m/z* 50-500.

153

154

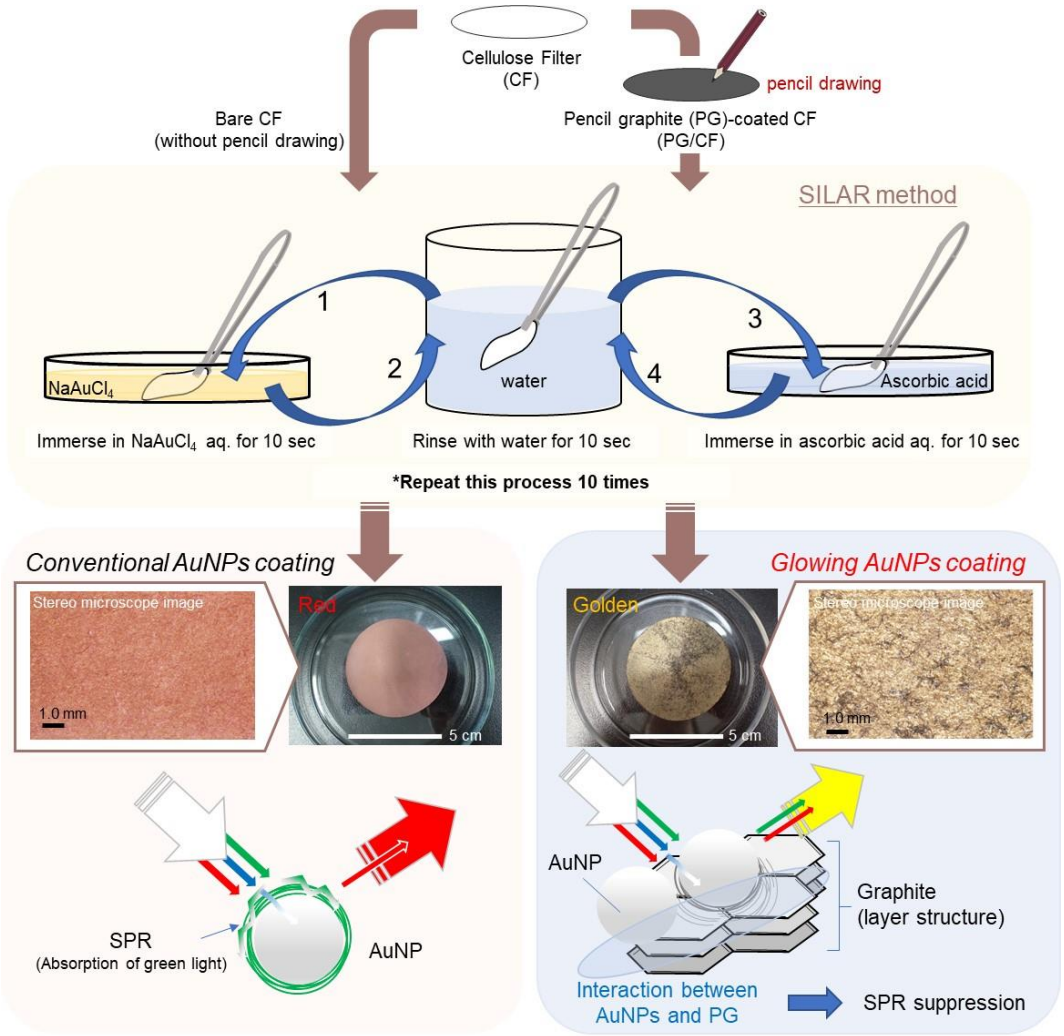

Fig. 1 Construction strategy of glowing AuNPs coating by combining the SILAR method with pencil drawing.

Results and discussion

A representative result was obtained by reducing Au (III) ions with ascorbic acid on/in PG-painted CF (Au/PG/CF) by the SILAR approach. As expected, the color of the treated surface was clearly a glowing golden color and the formation of the particles with the average diameter of 32 nm (n =

100) was observed without any aggregation (**Fig. 1, 2a and 2b**). The lattice fringes of the AuNPs were calculated to be 0.231 nm from a TEM image (**Fig. S1**), which is consistent with those of the Au (111) crystal plane (0.235 nm).[28] On the other hand, the average diameter of the AuNPs prepared on an intact CF (Au/CF) was 116 nm, and the color of the Au/CF was red-brown, which is a typical color of AuNPs based on the LSPR phenomenon (**Fig. 1, 2c and 2d**). The AuNPs of the Au/PG/CF were smaller and denser than those of the Au/CF (**Fig. S2**, $p < 0.01$; **Fig. 2b and 2d**), while these two samples did not show a significant difference in the gold content (**Table 1**).

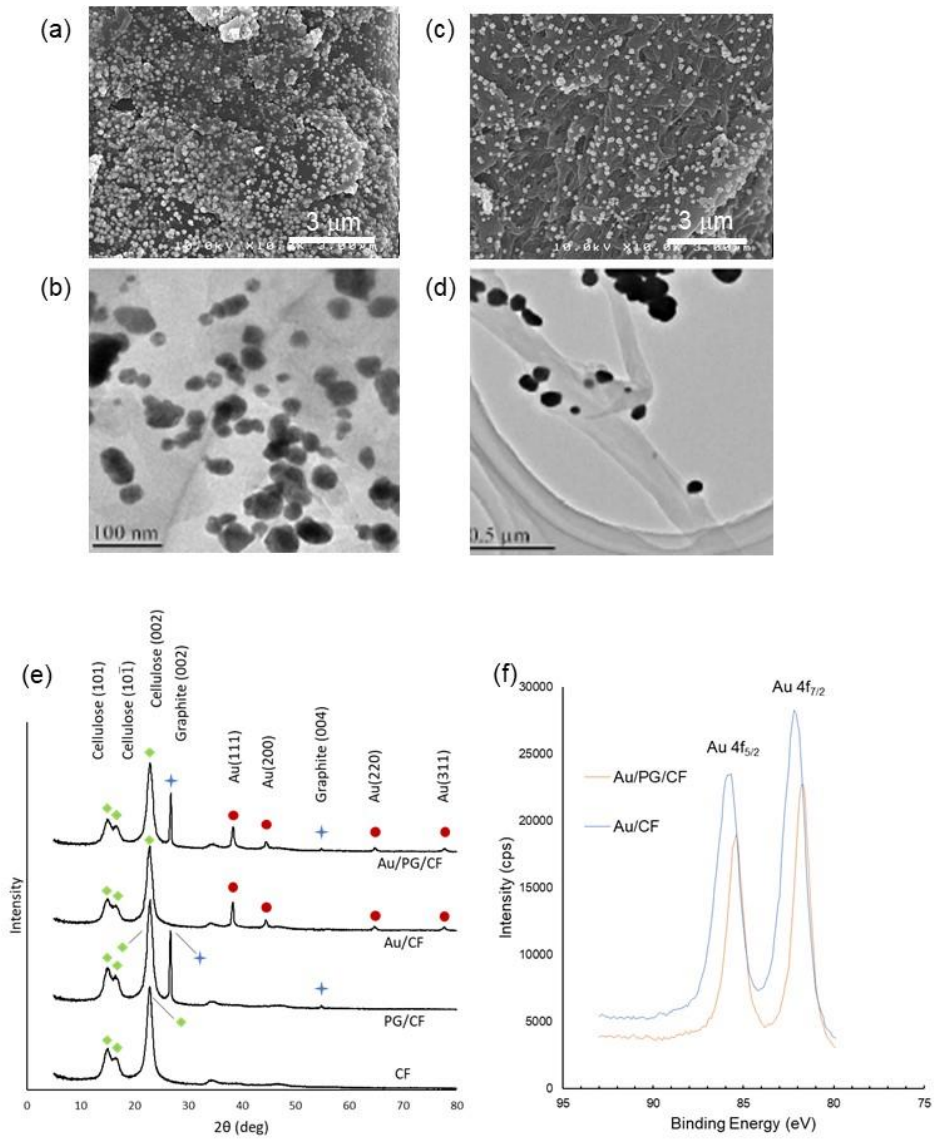

Fig. 2 (a,b) FE-SEM images and (c,d) TEM images of (a,c) the Au/PG/CF and (b,d) Au/CF. (e) XRD patterns of the CF, PG/CF, Au/CF, and Au/PG/CF. The peaks at around 34° correspond approximately to the (040) plane from the cellulose lattice. However, we could not determine the identification, because the peaks were broad. (f) Au 4f XPS spectra of the Au/PG/CF and Au/CF.

Table 1. Amount of attached PG and deposited AuNPs, diameter of the formed AuNPs, and electric resistivity of Au/CF, Au/PG/CF, PG/CF, and CF.

Sample	Au/CF	Au/PG/CF	PG/CF	Untreated CF
Attached amount of PG (mg/cm^2)	—	0.69	0.69	—
Deposited amount of Au (mg/cm^2)	0.147	0.155	—	—
Au particle diameter[a] (nm)	116 ± 24.5	32.2 ± 10.6	—	—
Electric resistivity $log_{10}(\Omega/\square)$	12[b]	3.7[b]	4.4[b]	>15[c]

[a] Diameter was calculated from TEM images (n=100).

[b] Statistically significant differences.

[c] The electric resistivity of the untreated CF was too high to determine by the high-resistivity meter.

For comparison, a bare CF or PG/CF immersed in the colloidal gold aqueous solution for one day was prepared, but they did not turn red or golden (data not shown), which shows that the alternate immersion in the SILAR process plays an important role in the AuNPs deposition on/in the CF substrate. X-ray diffraction (XRD) measurement also supported the fact that the target Au/PG/CF included all of the AuNPs, graphite, and CF from the peaks at 14.9°, 16.7°, and 22.8° corresponding to the (101), (10$\bar{1}$), and (002) planes from the cellulose lattice,[29] at 26.7° and 54.8° for graphite,[30] and at 38.2°, 44.6°, 64.7°, and 77.6° for the (111), (200), (220), and (311) planes of the gold crystals,[28] respectively (**Fig. 2e**).

In order to investigate the importance of graphite, the electric resistivities of CF, Au/CF, PG/CF, and Au/PG/CF were then evaluated (**Table 1**). The electric resistivity of the Au/PG/CF and PG/CF was much lower than those of CF and Au/CF, because of the electric conducting property of the

190 pencil graphite. It also seems that the presence of AuNPs contributed to the slight decrease in the
191 electric resistivity. Considering that the presence of PG drastically enhances the electric conductivity
192 of the materials and only the co-existence of AuNPs and PG provides the glowing golden coating,
193 the electron transfer between the AuNPs and PG of the Au/PG/CF might occur. X-ray photoelectron
194 spectroscopy (XPS) clearly supported that the $4f_{7/2}$ and $4f_{5/2}$ peaks of the Au/PG/CF were slightly
195 shifted to the lower binding energy compared to the peaks of the Au/CF, indicating the electron
196 transfer from the PG to AuNP (**Fig. 2f**). Similar results were reported for the Au/graphene hybrid
197 materials. [28,31] Taking such an electron transfer from the graphite to AuNPs into consideration, the
198 reason why the AuNPs of the Au/PG/CF were formed at a higher density compared to those of the
199 Au/CF might be because the crystal growth of AuNPs by the SILAR method would be suppressed by
200 the Coulomb repulsion between the AuNPs on the PG and $AuCl_4^-$.

201 When a carbon paper coating by carbon soot (elemental analysis; C: 87.67%, O: 8.08%, Cl:
202 4.25%) was used as a carrier of AuNPs instead of CF, the AuNPs on the carbon paper did not show
203 golden color. The electric resistivity of the carbon paper was high (>15 $\log_{10}(\Omega/\square)$), and the surface
204 of a carbon paper does not have layer structures as graphite. Furthermore, when graphene was
205 rubbed into CF as a carrier of AuNPs (electric resistivity of the sample: 3.8 $\log_{10}(\Omega/\square)$), only a small
206 part of the surface of the sample appeared golden color by the deposition of AuNPs. In the process of
207 rubbing graphene into CF, some graphene stacked, and layer structures would be formed partly.

208 These results indicate that the electron conductivity and layer structure of the PG/CF is needed for
209 the acquisition of the glowing property of AuNPs.

210 It is suggested that the AuNPs on the PG/CF interact with the graphite from the XPS results. In
211 addition, the electron conductivity of the Au/PG/CF was higher than that of the PG/CF (**Table 1**).
212 Based on these results, it is proposed that the AuNPs on the PG/CF take on the glowing property
213 through the possible mechanism as follows. The interaction between the AuNPs on the PG/CF and
214 the graphite builds out an electron network between the AuNPs. The electrons of the AuNPs behave
215 like free electrons of bulk gold through the network in the layer structure of the pencil graphite on
216 the cellulose filter. That leads the glowing property of the AuNPs on the PG/CF.

217 Another concern about the materials used in this study is the necessity of “CF” as a substrate
218 and “clay” in PG with various functional groups which would be the sites for the deposition of the
219 AuNPs. Thus, four materials, PG(6B)/CF (with less clay with more graphite with CF), graphite
220 powder (neither clay nor CF), PG powder (with clay without CF) and graphite/CF (without clay with
221 CF), were further evaluated as a substrate for the AuNPs. The obtained Au/PG(6B)/CF showed the
222 glowing golden color and the diameter of the AuNPs was about 100 nm, larger than that of the
223 Au/PG/CF and comparable to that of Au/CF (**Fig. S3**, **Table S1**).

224 The gold quantity of the Au/PG(6B)/CF was almost the same as that of the Au/CF or the
225 Au/PG/CF. The content of clay in the PG that influences the size of the AuNPs is not clear, but this

result clearly suggested that the particle size is not a decisive factor to determine the color of the AuNPs.

Further experiments have been performed to understand the influence of the size of AuNPs on the color of Au/PG/CF. There are several examples that the diameters of the nanoparticles formed by the SILAR method were changed by the initial concentrations of the metal ions in the solution for immersion.[26] When the concentration of $AuCl_4^-$ of the SILAR method was 1.0 or 10 mM, the color of the obtained Au/PG/CFs were also gold.

The quantities of the gold on the Au/PG/CFs were significantly increased by increasing the concentration of $AuCl_4^-$ (49 ± 21 μg cm^{-2} for 1.0 mM and 181± 4.9 μg cm^{-2} for 10 mM, n=5). The particle diameters were increased with the increase of the concentration of $AuCl_4^-$ (19.8± 6.5 nm for 1.0 mM and 68.9 ± 17 nm for 10 mM, $p<0.05$, n=100). There were no significant aggregations of AuNPs on the PG/CFs observed by TEM (data not shown). These results indicate that the diameter and quantity of the AuNP can be controlled by changing the Au concentration for the SILAR method.

Graphite powder or PG powder was directly employed in the SILAR method, but the AuNPs amount on/in their surfaces was much less than that of the Au/PG/CF possibly because of their surface hydrophobicity, and the obtained materials did not show a golden color (data not shown). Instead, the graphite powder was adhered by forcibly rubbing onto the CF to prepare the graphite/CF.

The SILAR method with graphite/CF as a substrate led to the glowing AuNP coating (**Fig. S4**), but the coated AuNPs (average diameter = 65 nm, n=100) as well as graphite easily detached from the material surface. These results clearly suggested that the combination of graphite and hydrophilic substrates (e.g., CF) is an effective way to accomplish the glowing AuNP coating, and clay would play an important role in anchoring the graphite/CF, AuNPs/graphite, and AuNPs/CF.

The hydrophilic property of the surface of a material would affect the deposition of nanoparticles by the SILAR method. The oxygen plasma treatment is one of the methods to improve the hydrophilic property of the surface of a material. It is well known that the surface of a carbon material was functionalized by polar groups and etched through the oxygen plasma treatment.[32] AuNPs were deposited on the plasma-treated PG/CF by the SILAR method ($NaAuCl_4$ aq., 5.0 mM). Interestingly, the color of the AuNPs on the plasma-treated PG/CF was not gold but red-brown. The result would be due to the disconnection of the network between the electrons of AuNPs and the graphite by the plasma etching and the modification of polar functional groups. The quantity of gold on the Au/PG/CF treated in plasma (0.113 mg cm^{-2}) was lower than that on the Au/PG/CF without the plasma treatment. This decrease would owe to the Coulomb repulsion between the $AuCl_4$ anion and the hydrophilic surface of the graphite formed by the plasma treatment.

The glowing AuNP coating could be simply localized by drawing a line or pattern with a pencil on the CF substrate, which is easily observed from the golden color on the drawn part and the

262 red-brown color on the bare part (**Fig. 3a-d**). Such a glowing coating was also applicable for fabrics
263 (polyester 65%, cotton 35%) in the same manner (**Fig. 3e and f**). On the other hand, the fabrics at
264 the part without pencil graphite was red. Interestingly, the AuNPs formed on the PG/fabrics showed
265 flower-like gold nanoparticles, observed by TEM (**Fig. 3h**). There were several nanoflower-type Au
266 nanoparticles at the part without pencil graphite (**Fig. 3g**), but these particles did not reveal golden
267 color. It has been reported that flower-like AuNPs on the reduced graphene oxide composite with
268 regenerated silk fibroin were synthesized.[33] It is not clear that this result was caused by the chemical
269 composition or surface features of the substrates, but different gold constructs might be formed by
270 applying this method to various substrates.

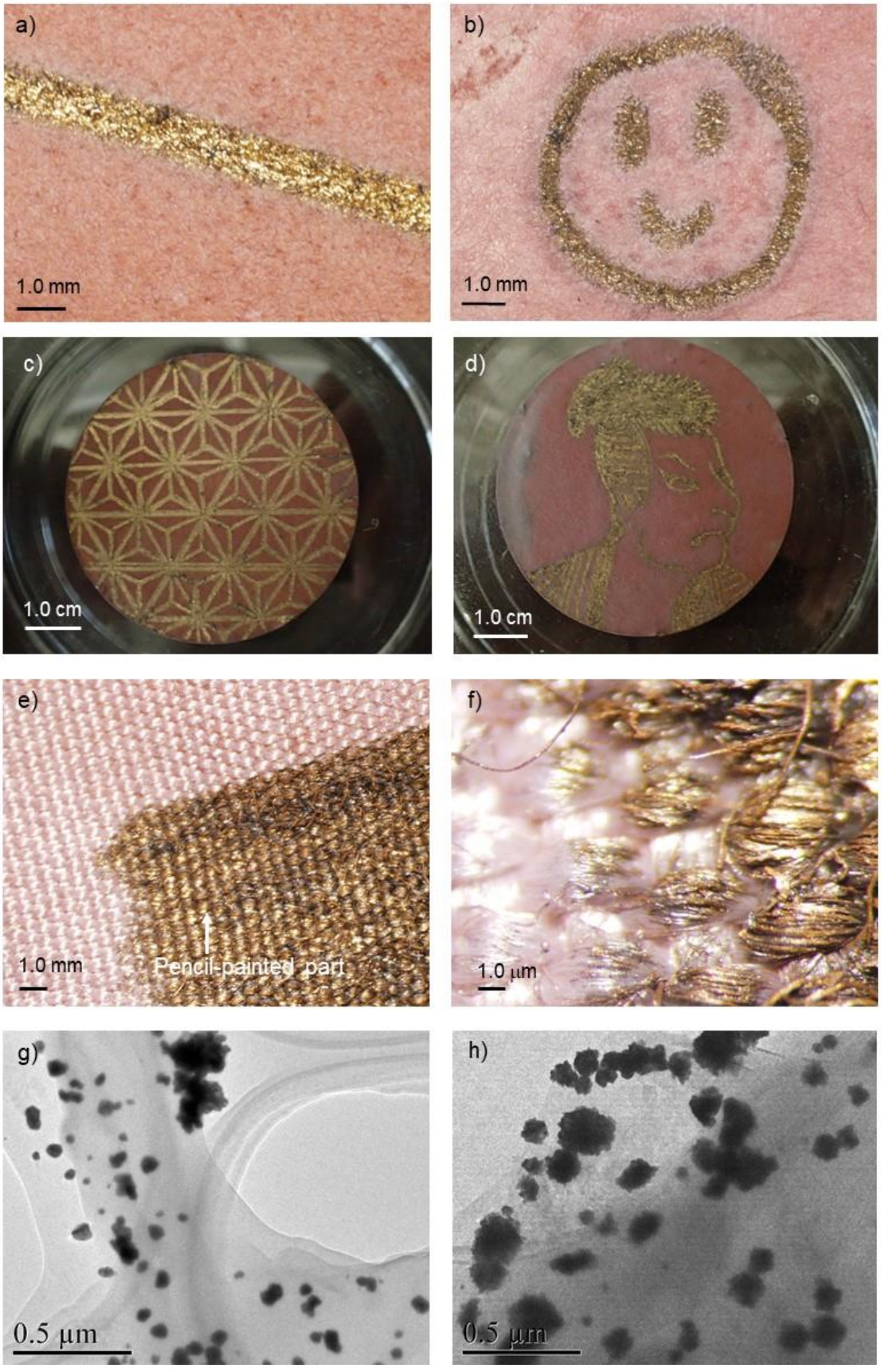
a)
1.0 mm
b)
1.0 mm
c)
1.0 cm
d)
1.0 cm
e)
1.0 mm
Pencil-painted part
f)
1.0 μm
g)
0.5 μm
h)
0.5 μm

271

272 **Fig. 3** Fabrication of controlled glowing AuNP patterns by pencil drawing. (a) Line, (b) Smiley, (c)

273 "Asanoha" pattern, and (d) "Ukiyo-e" prepared on CF. (e,f) Glowing fabric/fibers (PET/cotton). (g,

274 h) TEM image of AuNPs formed on the fabrics/fibers without pencil graphite for (g) and with pencil

275 graphite for (h).

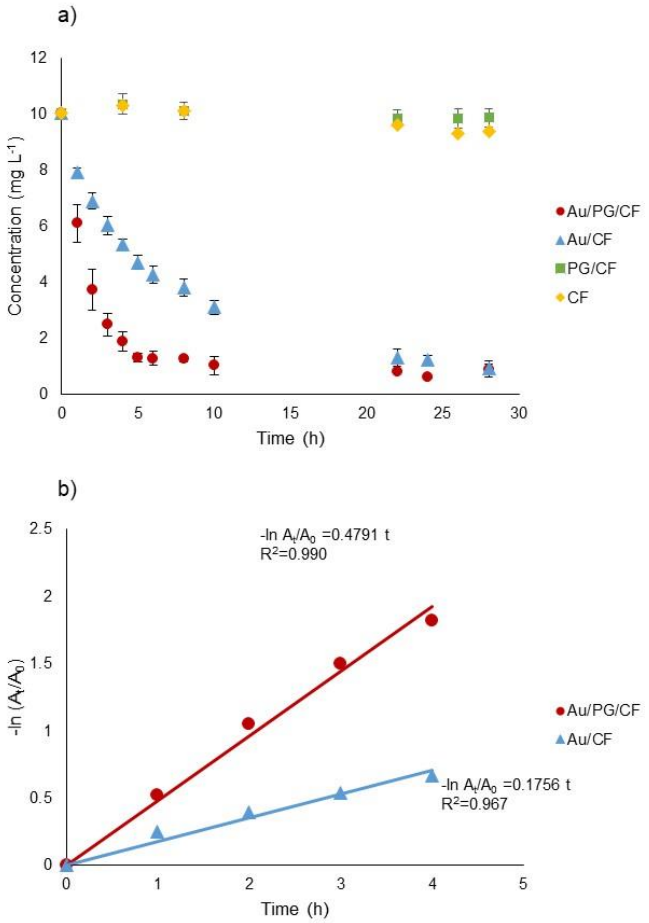

276

277 **Fig. 4** Reduction of *p*-NP with $NaBH_4$ in the presence of Au/PG/CF, Au/CF, PG/CF, and CF. (a)

278 Remaining concentration of *p*-NP with reaction time (n=3). (b) Pseudo-first order plots of the

279 degradation of *p*-NP vs reaction time. A_0 is the initial absorbance at 400 nm, and A_t is the absorbance

280 at t h.

281 The golden AuNPs and red-brown AuNPs should show different chemical and physical
282 properties because of their different electronic and optical properties. It is well known that the
283 catalytic activity of the AuNPs is affected by the particle size and the kind of substances supporting
284 the AuNPs.[30,34,35] Haruta *et al.* reported that AuNPs attached onto metal oxides exhibited a catalytic
285 activity for the oxidation of carbon oxide at room temperature.[36,37] Since then, various catalytic
286 reactions using AuNPs have been developed, and some of them are industrially used.[38] Herein, as a
287 model reaction, the reduction of *p*-nitrophenol (*p*-NP) to *p*-aminophenol (*p*-AP) with $NaBH_4$ as a
288 reducing agent in the presence of AuNPs was tested. In the case of the reaction using the Au/CF or
289 the Au/PG/CF, the concentration of *p*-NP decreased with time, while the reaction did not occur by
290 using the untreated CF and the PG/CF without AuNPs as the negative controls (**Fig. 4a**). The plot of
291 $-\ln A_t/A_0$ versus time shows an approximate linearity for both Au/PG/CF and Au/CF, indicating that
292 the reduction of *p*-NP in the presence of the AuNP-coated filters fitted a pseudo-first-order kinetic
293 model and the rate constant of the reaction using the Au/PG/CF was about 2.5 times that using the
294 Au/CF. (**Fig. 4b**).

295 In general, a decrease of the particle size of AuNPs leads to an increase of the catalytic
296 activity.[34,35] The catalytic activity of Au/PG/CF was higher than that of Au/CF. In addition, the
297 average diameter of AuNPs on the PG/CF was smaller than that of Au/CF (**Table 1**), and the
298 significant aggregation of AuNPs was not observe by the FE-SEM and TEM measurements. Based

299 on these results, it is suggested that the glowing property of the AuNPs on the PG/CF is not due to
300 the aggregation of AuNPs.

301 The catalytic activity of Au/PG(6B)/CF was comparable to that of Au/CF (**Fig. S5**), and thus it
302 would be reasonable to consider that the increased activity might be caused by both the size effect
303 and electronic properties of the AuNPs. The catalytic activity of Au/PG/CF could also be applied for
304 the detoxification of aromatic nitro compounds[10], that is, the reduction of pendimethalin and
305 2,4-dinitrophenol, herbicides containing two nitro groups (**Fig. S6** for pendimethalin).

306

307 Conclusion

308 In summary, we successfully developed an easy and powerful approach for realizing the glowing
309 AuNP coating by combining the SILAR method with PG drawing, and showed some requirements,
310 such as hydrophilic substrates (e.g., CF, fabrics), graphite/clay composite (e.g., PG), and crystal
311 growth of Au(III) on the substrate (e.g., SILAR method). The reason why the prepared surfaces
312 showed the golden color is not totally understood, but electronic resistivity and XPS measurements
313 suggested that the free electrons of the AuNPs of the Au/PG/CF might behave like those of the bulk
314 gold due to the 3-dimensional electron transfer between the AuNPs and graphite. In addition, the
315 AuNPs prepared in this study showed a significant catalytic activity possibly because of such a
316 strange electronic property as well as the large surface area. We believe that such glowing AuNPs

revived the lost property of the bulk gold that would lead to further advancement in the arts and culture as well as electronics, optics, and catalysis. The presented method may not only inspire further development of novel AuNP materials, but also could lead to the development of materials using the other metal nanoparticles.

Acknowledgements

This work was partly supported by JSPS KAKENHI Grant Number 17K00625.

Notes and references

1 J. Jeevanandam, A. Barhoum, Y. S. Chan, A. Dufresne, M. K. Danquah, *Beilstein J. Nanotechnol.,* 2018, **9**, 1050–1074.

2 H. Chen, L. Su, M. Jiang, X. Fang, *Adv. Funct. Mater.*, 2017, **27**, 1704181.

3 S. Campione, C. Guclu, R. Ragan, F. Capolino, *ACS Photonics*, 2014, **1**, 254–260.

4 D. Iqbal, A. Sarfraz, A. Erbe, *Nanoscale Horiz.*, 2018, **3**, 58–65.

5 K. D. Gilroy, A. O. Elnabawy, T. H. Yang, L. T. Roling, J. Howe, M. Mavrikakis, Y. Xia, *Nano Lett.*, 2017, **17**, 3655–3661.

6 Z. Jia, M. B. Amar, D. Yang, O. Brinza, A. Kanaev, X. Duten, A. V. González, *Chem. Eng. J.*, 2018, **347**, 913–922.

7 K. Murata, Y. Mahara, J. Ohyama, Y. Yamamoto, S. Arai, A. Satsuma, *Angew. Chem. Int. Ed.,* 2017, **56**, 15993–15997.

8 S. A. Aromal, D. Philip, *Phys. E: Low-dimensional Syst. Nanostruct.*, 2012, **44**, 1692–1696.

9 Y. Wu, G. Li, J. P. Camden, *Chem. Rev.,* 2018, **118**, 2994–3031.

10 K. Mao, Y. Chen, Z. Wu, X. Zhou, A. Shen, J. Hu, *J. Agric. Food Chem.*, 2014, **62**, 10638–10645.

11 H. Kawasaki, T. Sugitani, T. Watanabe, T. Yonezawa, H. Moriwaki, R. Arakawa, *Anal. Chem.*, 2008, **80**, 7524–7533.

12 J. P. Leung, S. Wu, K. C. Chou, R. Signorell, *Nanomaterials*, 2013, **3**, 86–106.

13 Z. Ebrahimpour, N. Mansour, *Plasmonics*, 2018, **13**, 1335–1342.

14 A. Buccolieria, E. R. Cesareoc, A. Castellanod, G. Buccolierid, *Measurement*, 2018, **126**, 164–167.

15 S. S. Shankar, A. Rai, A. Ahmad, M. Sastry, *Chem. Mater.*, 2005, **17**, 566–572.

16 M. C. Daniel, D. Astruc, *Chem. Rev.*, 2004, **104**, 293–346.

17 A. S. Nair, T. Pradeep, *J. Nanosci. Nanotechnol.*, 2007, **7**, 1871–1877.

18 T. Ung, L. M. L. Marzan, P. Mulvaney, *J. Phys. Chem. B*, 2001, **105**, 3441–3452.

19 M. Torrell, P. Machado, L. Cunha, N. M. Figueiredo, J. C. Oliveira, C. Louro, F. Vaz, *Surf. Coat. Technol.,* 2010, **204**, 1569–1575.

20 M. Torrell, L. Cunha, M. R. Kabir, A. Cavaleiro, M. I. Vasilevskiy, F. Vaz, *Mater. Lett.*, 2010, **64**, 2624–2626.

21 V. Amendola, G. A. Rizzi, S. Polizzi, M. Meneghetti, *J. Phys. Chem. B*, 2005, **109**, 23125–23128.

22 K. Ariga, Y. Yamauchi, G. Rydzek, Q. Ji, Y. Yonamine, K. C. W. Wu, J. P. Hill, *Chem. Lett.*, 2014, **43**, 36–68.

23 G. Popa, F. Boulmedais, P. Zhao, J. Hemmerle, L. Vidal, E. Mathieu, O. Lix, P. Schaaf, G. Decher, J. C. Voegel, *ACS Nano*, 2010, **4**, 4792–4798.

24 R. K. Iler, *J. Colloid Inter. Sci.*, 1996, **21**, 569–594.

25 T. Taguchi, A. Kishida, M. Akashi, *Chem. Lett.*, 1998, **8**, 711–712.

26 W. Kim, J. C. Lee, G. J. Lee, H. K. Park, A. Lee, S. Choi, *Anal. Chem.*, 2017, **89**, 6448–6454.

27 M. C. Sousa, J. W. Buchanan, *Computer Graphics forum*, 2000, **19**, 27–49.

28 J. Li, C. Liu, Y. Liu, *J. Mater. Chem.*, 2012, **22**, 8426–8430.

29 C. J. Garvey, I. H. Parker, G. P. Simon, *Macromol. Chem. Phys.*, 2005, **206**, 1568–1575.

30 G. Sun, X. Li, Y. Qu, X. Wang, H. Yan, Y. Zhang, *Mater. Lett.*, 2008, **62**, 703–706.

31 S. Y. Jeong, S. H. Kim, J. T. Han, H. J. Jeong, S. Y. Jeong, G. W. Lee, *Adv. Funct. Mater.*, 2012, **22**, 3307–3314.

32 U. Cvelbar, S. Pejovnik, M. Mozetiè, A. Zalar, *Appl. Sur. Sci.*, 2003, **210**, 255–261.

33 S. Xu, L. Yong, P. Wu, *ACS Appl. Mater. Inter.*, 2013, **5**, 654–662.

34 K. Shimizu, Y. Miyamoto, T. Kawasaki, T. Tanji, Y. Tai, A. Satsuma, *J. Phys. Chem. C*, 2009, **113**, 17803–17810.

35 H. Chen, H. Kang, Y. Gong, J. Guo, H. Zhang, R. Liu, *ACS. Appl. Mater. Inter.*, 2015, **7**, 21717–21726.

36 M. Haruta, *Catalysis Today*, 1997, **36**, 153–166.

37 M. Haruta, *Angew. Chem. Int. Ed.*, 2014, **53**, 52–56.

38 T. Hayashi, K. Tanaka, M. Haruta, *J. Catalysis*, 1998, **178**, 566–575.